

Starch–Chitosan Blend Cross-Linked with Calcium Chloride



Jaya Maitra and Neena Singh

Abstract In this research, different compositions of starch and chitosan blends are prepared by cross-linking with calcium chloride. Starch and chitosan ratios are fixed, i.e., 10:10 mL and the calcium chloride concentration varies between 0.8 and 2.4 mL (0.8, 1.2, 1.6, 2.0, and 2.4 mL). Totally five samples are prepared. Prepared blends were characterized by FTIR, SEM, and TGA Swelling behavior of the prepared blends is observed. The results showed that at 2.0 mL concentration of calcium chloride, the blend showed the highest swelling behavior. Antibacterial property of the same blend having 2.0 mL concentration of calcium chloride was studied against *Escherichia coli*.

Keywords Blend · Chitosan · Cross-linking · Calcium chloride

1 Introduction

Chitosan and starch both are biodegradable, nontoxic, hydrophilic and biocompatible polymer [1]. Chitosan is a natural polysaccharide formed during the deacetylation of chitin in alkaline condition. It has antimicrobial property and excellent film-forming ability, which makes it suitable for obtaining antimicrobial films [2]. It has wide application in pharmaceutical, medical, and cosmetic industries due to its positive electrical charge which allows it to combine with negative electrical charge of skin and hair [3]. It is used in shampoos, hair gels, tooth paste, mouth wash, and skin care products [4]. Because of its biological properties, biodegradability, bioactivity, and biocompatibility, it has attracted much attention in the field of biomaterials, food coating, and packaging industry [5, 6]. The drawback associated with chitosan hydrogels is relatively low mechanical strength due to its hydrophilic nature and greater solubility in acidic medium.

J. Maitra (✉) · N. Singh
Department of Applied Chemistry, School of Vocational Studies
and Applied Sciences, Gautam Buddha University, Greater Noida, India
e-mail: jaya@gbu.com

© Springer Nature Singapore Pte Ltd. 2018
B. Gupta et al. (eds.), *Advances in Polymer Sciences and Technology*,
Materials Horizons: From Nature to Nanomaterials,
https://doi.org/10.1007/978-981-13-2568-7_13

The other natural polymer is starch which is most abundant, cheap, biodegradable, and renewable, i.e., it can be regenerated from carbon dioxide and water by photosynthesis in plants [7–9]. It is a semi-crystalline polymer, composed of two repeating units of 1, 4- α -D-glucopyranosyl: amylose and amylopectin. Starch has different proportions of amylose and amylopectin ranging from about 10–20% amylose and 80–90% amylopectin [10]. It is hydrophilic in nature. The drawback associated with articles prepared from starch and water is their brittleness and sensitivity to atmospheric moisture [11].

Complimentary nature of chitosan and starch has attracted considerable attention in the areas such as biotechnology, biomedicine, food ingredients, and cosmetics [12, 13]. Hydrogels of chitosan and starch are widely used for various purposes such as drug delivery and tissue engineering systems [14].

2 Experimental Setup: Preparation of Starch–Chitosan Blends/Films

2.1 Polymers and Reagents

Chitosan from HiMedia, Acetic acid glacial, free aldehyde.A.R. from HiMedia, Calcium chloride from HiMedia, Starch, from Titan Biotech Ltd.

2.2 Preparation of Chitosan–Starch and Calcium Chloride Solutions

Stock of 1% (v/v) acetic acid aqueous solution was prepared by dissolving 1 mL acetic acid in 99 mL distill water. Chitosan solution (2% w/v) was prepared by dissolving 2 gm of chitosan in 100 mL of 1% acetic acid aqueous solution with the help of magnetic stirrer. 2% (w/v) starch solution was also prepared by dissolving 2 g of starch in 1% acetic acid aqueous solution. Solvent for the chitosan and starch was the same. Calcium chloride 2% (w/v) aqueous solution was prepared by dissolving the 2 mL calcium chloride in 100 mL distill water.

2.3 Preparation of Chitosan–Starch Films Cross-Linked with Calcium Chloride

Five different samples of starch and chitosan are prepared. All the samples contains fixed ratios of starch and chitosan, i.e., 10 mL each and change the volume calcium chloride, i.e., 0.8, 1.2, 1.6, 2.0, and 2.4 mL. Different ratios of calcium chloride are

added dropwise into starch and chitosan (10:10 mL) blend with continuous stirring at 600 rpm. After that, the blends are poured in the Petri plates and set aside at room temperature for drying. After drying, thin films are placed in hot air oven at 25–30 °C for 15 min and then placed at room temperature. Resulting dried films are stored in plastic poly bags.

3 Characterization

The surface morphology of the prepared film is observed by exploring the microstructures through the Scanning Electron Microscopy (SEM). Prepared films are also characterized by Fourier-Transform Infrared Spectroscopy (FTIR) and Thermogravimetric analysis (TGA).

3.1 Fourier-Transform Infrared (FTIR) Studies

FT-IR analyses of starch–chitosan-blended films cross-linked with CaCl₂ is measured in the wave number range 500–4000 cm⁻¹ (Tables 1, 2, and 3).

FTIR spectrum of pure chitosan Fig. 1 (A1) shows a broad band in vibration spectrum due to stretching vibrations of OH groups in the range from 3744 to 3000 cm⁻¹ [ν_{OH}], which are overlapped to the stretching vibration of N–H (3500–3000 cm⁻¹); and C–H bond in –CH₂ ($\nu_1 = 2920$ cm⁻¹) and –CH₃ ($\nu_2 = 2875$ cm⁻¹) groups,

Table 1 FTIR peaks positions for starch

S. No.	Peak (cm ⁻¹)	Functional group
1	3000–3600	– OH Str.
2	2800–3000	– CH ₂ deformation
3	1642	Presence of water in the amorphous region of structure
4	1415	CH ₂ bending and COO-Str
5	1344	C–OH bending and CH ₂ twisting
6	1242	CH ₂ OH (side chain) related mode
7	1163	C–O and C–C str.
8	1094	C–OH bending
9	1067	C–H bending
10	930	α 1–4 glycosidic linkage
11	764	C–C str.
12	537	Skeletal mode of pyranose ring

Table 2 FTIR peaks positions for chitosan

S. No.	Peak (cm ⁻¹)	Functional group
1	3007–3744	– OH/NH vibrations
3	2880	– C–H stretching (reduced)
4	2356	Symmetric and asymmetric C–H vibrations
5	1650	1650–1660 cm ⁻¹ amide I/–NH ₃ ⁺ str
6	1560	N–H bending peak
7	1458	– H ₂ C–N– str. (amide group)
8	1260	C–N vibration
9	1154	C–O stretching bend
10	1097	C–O–C stretching/water molecule present in chitosan
11	1028	C–O–C stretching

Table 3 FTIR peaks positions for chitosan

S. No.	Peak (cm ⁻¹)	Functional group
1	2800	– C–H stretching symmetric and asymmetric
2	1759	– C=O interaction with Ca ⁺⁺
3	1650–1660	Amide I Stretch in (CONH ₂)
4	1458	– CONH str.
5	1260	C–N vibration
6	1154	C–O bend

respectively. A broad absorption in the range of 1654–1260 cm⁻¹ [$\nu_{C=O}$] is due to the vibrations of carbonyl bonds of the amide group CONHR (secondary amide, $\nu_1 = 1645$ cm⁻¹) and vibrations of protonated amine group (δ_{NH_3} , $\nu_2 = 1574$ cm⁻¹). The presence of CH₂ can be also confirmed from the presence of bending vibrations of methylene and methyl groups were also visible at $\nu = 1375$ cm⁻¹ and $\nu = 1426$ cm⁻¹, respectively. Absorption in the range from 1154 to 1000 cm⁻¹ has been attributed to the vibrations of CO group. The band located near $\nu = 1154$ cm⁻¹ is related to asymmetric vibrations of CO in the oxygen bridge resulting from deacetylation of chitosan. The bands near 1080–1025 cm⁻¹ are attributed to ν_{CO} of the ring C–OH, C–O–C and CH₂OH. The small peak at ~890 cm⁻¹ corresponds to wagging of the saccharide structure of chitosan.

Figure 1(A2) shows the FTIR spectra of starch. O–H stretching mode of starch was between 3000 and 3600 cm in the spectrum. The C–H stretching modes were observed in the 2800–3000 cm⁻¹ region. Bands at 2922 and 2856 cm⁻¹ depict the CH₂ deformation band of methylene hydrogen atom. On the other hand, a band at 1415 cm⁻¹ is assigned to CH₂ bending or C–O–O stretching band of starch subunit.

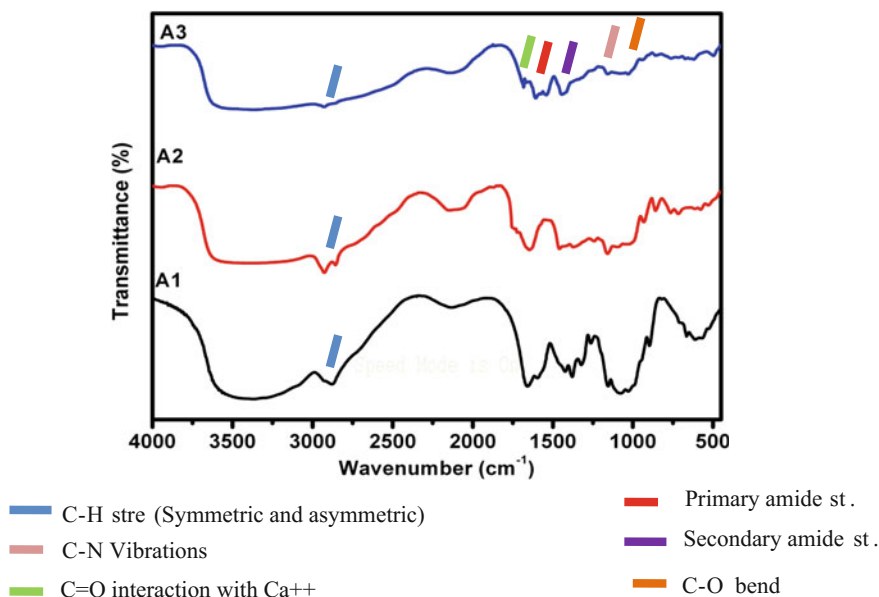


Fig. 1 FTIR of soluble chitosan (A1), starch (A2), and blend (A3)

Similarly, bands at 1259 and 1095 cm^{-1} can be assigned to CH_2OH (side chain) related and C–O–H bending mode, respectively. The band at 1743 cm^{-1} in the spectrum of starch was assigned to stretching vibrations of carbonyl groups ($\nu_{\text{C}=\text{O}}$). The appearance of band at 1643 cm^{-1} shows characteristic IR band of tightly bound H_2O molecules to the starch chain. The vibrations originating from the C–O–C of R-1,4 glycosidic linkages could be observed as a strong Raman band in the vicinity of 920–960 cm^{-1} . The major bands at 647 cm^{-1} and minor bands between 560 and 400 cm^{-1} can be attributed to the skeletal modes of the pyranose ring.

Figure 1(A3) shows the FTIR spectra of starch–chitosan blend cross-linked with calcium chloride. The peak at 2800 cm^{-1} for C–H stretching symmetric and asymmetric. The weak peak at about 1790 cm^{-1} is due to the C=O bonding of Ca^{++} . Peaks around 1650–1660 cm^{-1} show the C–N stretch of amide I. Peaks around 1458 cm^{-1} show the stretch of amide II. Peaks around 1238 cm^{-1} show the C–N vibrations. Peaks around 1157 cm^{-1} show the C–O bending. The peaks from 600 to 1400 cm^{-1} can be attributed to the C–O, C–C, and C–N bonding of chitosan and Ca^{++} .

4 Scanning Electron Microscopy

The scanning electron microscopy (SEM) of the prepared film from the blending of starch and chitosan and cross-linked with CaCl_2 have been analyzed by Carl Zeiss EVO-50.

Surface morphology of the films is characterized by SEM at the magnification of 10 μm . Figure 2 shows the SEM microstructures of starch film (A) and starch and chitosan blend cross-linked with calcium chloride (B). The surface of starch film is rough and contains non-dissolved lumps on the surface. Microstructure observations demonstrated that inclusion of chitosan concentration with the starch (for a blend) leads to the formation of fine surface. The surfaces of chitosan and starch blended film is homogenous and nonporous, it demonstrates the uniform distribution of chitosan and starch molecules all over the films, which predict the hydrogen bonds/ionic bonds between the functional groups of the chitosan and starch, i.e., $-\text{OH}$ and $-\text{NH}_2$ groups in chitosan and $-\text{OH}$ groups in starch (Fig. 2). The morphology of the starch–chitosan-blended film cross-linked with CaCl_2 demonstrated that addition of chitosan to the starch and cross-linking with CaCl_2 improved the surface morphology of the film and lessening the non-dissolved lumps on the surface of the film, which predict the interaction between chitosan, starch, and calcium chloride.

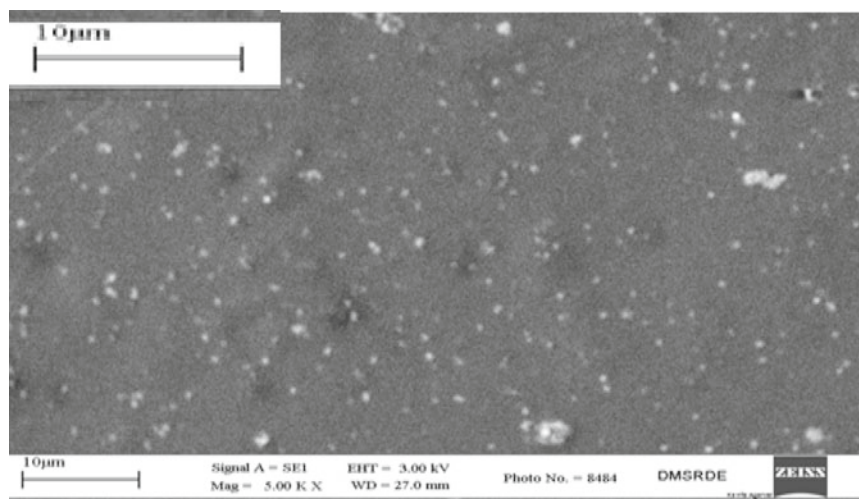
5 Thermogravimetric Analysis (TGA)

TGA thermograms of starch–chitosan blend cross-linked with calcium chloride (in the temperature range 0–500 $^\circ\text{C}$ under nitrogen) are shown in Fig. 3.

5.1 TGA of Pure Chitosan

Thermal details (TGA) of 75% deacetylated chitosan are shown in Table 4 and Fig. 3. Figure 3 shows that 10% decomposition of pure chitosan takes place at 130 $^\circ\text{C}$ while 20, 30, 40, 50, and 60% decomposition of chitosan takes place at 235, 275, 287, 320, and 415 $^\circ\text{C}$, respectively.

Figure 3 also shows the two consecutive weight loss steps in the pure chitosan. The first weight loss was 12% in the range of 75–130 $^\circ\text{C}$ temperature, which was accountable for the loss of moisture content and demonstrated the hygroscopic nature of the chitosan. The second weight loss from 20 to 50% in the range of 235–320 $^\circ\text{C}$, which was due to breakage of ether linkage in the chitosan backbone. The weight loss of 66% in the range of 415–500 $^\circ\text{C}$ predicts the thermal decomposition of glucosamine units.



A=Starch film



B=Starch-Chitosan blend with CaCl₂

Fig. 2 Microstructures of starch (a) and blend with calcium chloride (b)

5.2 TGA of Pure Starch

Thermal details (TGA) of pure starch is given in Table 5 and Fig. 3. Figure 3 shows that 10% decomposition of pure starch takes place at 163 °C while 20, 30, 40, 50,

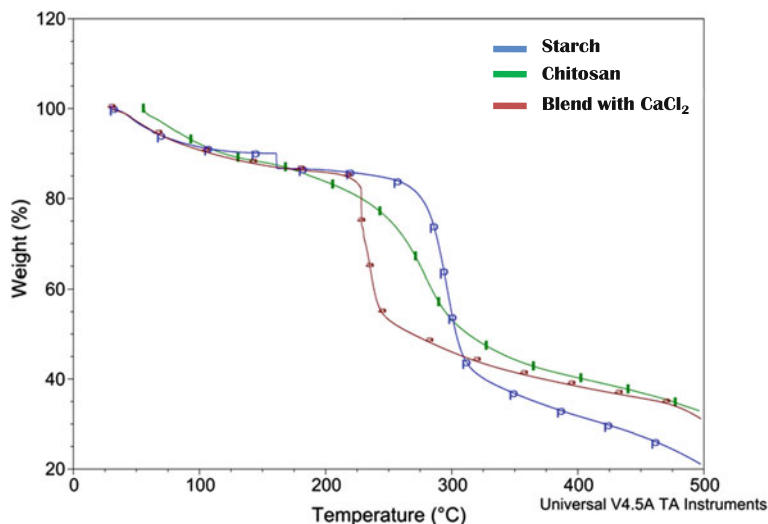


Fig. 3 TGA thermogram of pure chitosan

Table 4 TGA of pure chitosan

Percentage decomposition (%)	Decomposition temperature (°C)
10	130
20	235
30	275
40	287
50	320
60	415
66	500

60, and 70% decomposition of starch takes place at 285, 299, 302, 310, 330, and 415 °C respectively.

Figure 3 shows the three consecutive weight loss steps in the pure starch. The first weight loss was at 163 °C. Almost 10% weight loss at temperature 163 °C is accountable for the loss of moisture content and demonstrated the hygroscopic nature of starch. The second steep weight loss from 20 to 40% in the range of 285–302 °C is due to the dehydration of the saccharide rings and depolymerization. Degradation between the range of 310–330 °C is attributed to the degradation of starch components, i.e., amylose and amylopectin. Amylose degrades first because of its straight chain structure. A thermal reaction of condensation between hydroxyl groups and dehydration of neighboring hydroxyl group in the glucose ring (causing ring scission) starts at 300 °C. In the third stage, the weight loss was started at the temperature 415 °C onwards, and until the temperature 500 °C the weight loss was

Table 5 TGA of pure starch

Percentage decomposition (%)	Decomposition temperature (°C)
10	163
20	285
30	299
40	302
50	310
60	330
70	415
79	500

Table 6 TGA of chitosan–starch blend cross-linked with CaCl₂

Percentage decomposition (%)	Decomposition temperature (°C)
10	110
20	231
30	232
40	237
50	270
60	377
70	498

79% which predicts the thermal decomposition thermal decomposition of glucose residues.

5.3 TGA of Starch–Chitosan Blend Cross-Linked with CaCl₂

Thermal details (TGA) of chitosan–starch blend crosslinked with CaCl₂ are shown in Table 6. Figure 3 shows the 10% decomposition of chitosan–starch blend cross-linked with CaCl₂ takes place at 110 °C while 20, 30, 40, 50, 60, and 70 decomposition of starch takes place at 231, 232, 237, 270, 377, and 498 °C, respectively

Figure 3 shows the two consecutive weight loss steps in the chitosan–starch blend cross-linked with CaCl₂. The first weight loss was 10–16% at 30–225 °C temperature, which was accountable for the loss of moisture content and demonstrated the hygroscopic nature of the blend. Suddenly, a steep loss of 54.5 wt% in the range of 231–272 °C temperature was observed which was due to cleavage of the ionic linkage. The second weight loss was at 400 °C and the total weight loss until this temperature is 62%, which predicts the thermal decomposition of glucosamine residues. At the temperature 500 °C, the total weight loss was 68%.

Table 7 Rate of thermal decomposition (%) of chitosan, starch, and blend with calcium chloride

Temperature (°C)	Chitosan % weight loss	Starch % weight loss	Blend % weight loss
100	7	8	8
200	18	12	14
300	45	34	54
400	58	68	62
500	66	79	68

Table 7 and Fig. 3 represent the TGA thermogram details of pure chitosan, pure starch, and starch–chitosan (10:10) blend cross-linked with CaCl_2 . Figure 3 shows the chitosan decomposes the least at 100 °C, i.e., 7% while blend and starch decompose 8% of their weight while at 500 °C chitosan decomposes 66% and blend decomposes 68% of its weight which shows that the blend is quite stable with respect to its parent material chitosan and starch.

6 Swelling Property

The % swelling ratios of the films are measured. The known weight, i.e., W_d of each film are immersed into the distill water at room temperature one hours. After one hour, films are removed from the distill water and are weighed, i.e., W_s . The % swelling ratio of the films are calculated by using equation,

$$E = [(W_s - W_d) / W_d] \times 100$$

where

E percent swelling ratio;

W_d weight of film in dry state;

W_s weight of film in swollen state.

The swelling behavior of starch and chitosan-blended films as shown in Fig. 4 increases as the calcium chloride ratio increase up to 2 mL of 2% CaCl_2 solution is added into starch–chitosan blend and it gives the highest swelling behavior at 2 mL concentration of calcium chloride as shown in Table 8 and Fig. 4. After that, suddenly the films containing 2.4 mL solution of calcium chloride shows decline in the swelling behavior.

Fig. 4 Swelling behavior of starch–chitosan films (cross-linked with calcium chloride)

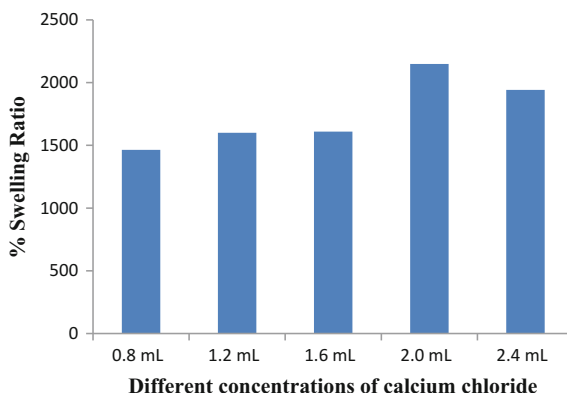


Table 8 % swelling ratio of starch–chitosan-blended films cross-linked with calcium chloride

St: Chi + CaCl ₂ (mL)	Dry Wt. (g)	Wet Wt. (g)	Wet–Dry Wt. (g)	% swelling $E = [(W_s - W_d) / W_d] \times 100$
10:10 + 0.	0.072	1.126	1.054	1463.88
10:10 + 1.2	0.034	0.578	0.544	1600.00
10:10 + 1.6	0.064	1.094	1.030	1609.375
10:10 + 2.0	0.061	1.372	1.311	2149.18
10:10 + 2.4	0.024	0.490	0.466	1941.66

7 Antibacterial Assay

Disc diffusion method is used to check the antibacterial property of the blend. LB agar Petri plates are prepared by dissolving the 2.5 g of LB and 2 g of agar in 100 mL distill water. After autoclaving at 120 °C, 25 mL of solution was poured in one Petri plate in slight warm condition. Over night grown culture of *Escherichia coli* is diluted to 10^{-4} dilution and 20 μ L of the diluted culture is spread on the Petri plate of size 90 \times 15 mm. 6 mm sized discs are placed in the petriplate. 15 μ L of the starch–chitosan cross-linked with CaCl₂ blend (2 mL of 2% CaCl₂ is applied on 6 mm size disc A. Petri plates are placed in incubator at 37 °C and zone of inhibitions are observed after 24 h.

7.1 Antibacterial Activity of Polymeric Blend

The ionic cross-linking of starch–chitosan-blend with cross-linker 2 mL of 2% CaCl₂ shows zone of inhibition of 6.4 mm in diameter, supporting the antibacterial activity of the blend against *E. coli* (Figs. 5 and 6).

Fig. 5 LB Agar plate of *E. coli*

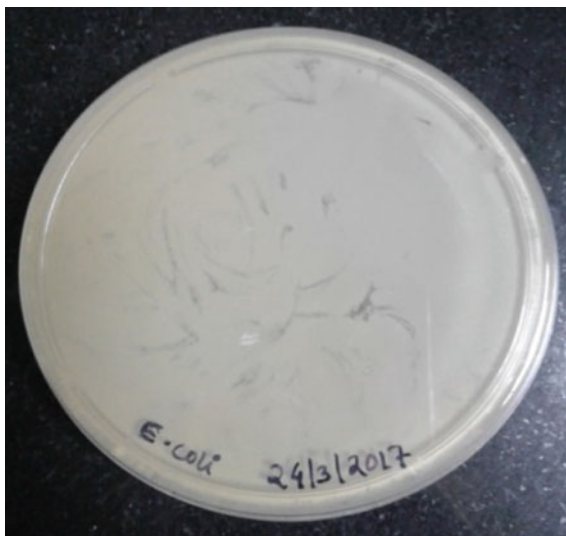


Fig. 6 Antibacterial activity of blend against *E. coli*



8 Conclusion

Present research is based on the development of starch and chitosan-based biodegradable films for the biomedical, pharmaceutical, and packaging purposes. The blend of starch and chitosan is cross-linked with calcium chloride is prepared. Prepared blend is characterized by Fourier-Transform Infrared (FTIR), Scanning Electron Microscopy (SEM), and Thermogravimetry Analysis (TGA). The results of FTIR studies demonstrated the peak at 1790 cm^{-1} , which shows the C=O bonding with Ca^{++} and the reduced peak intensity of the blend between the range 600 and

1400 cm^{-1} which further confirms the interaction of Ca^{++} with C–O, C–C, and C–N of chitosan.

SEM microstructures studies of the blend demonstrating the smooth surface with reduced non-dissolved granules of the starch at the surface of the pure starch film further confirms the interaction between starch, chitosan, and CaCl_2 . Thermogravimetry Analysis (TGA) explains the degradation of blend at the higher temperature, which again supports the blending of the constituents and supports that the blend is thermally stable.

Swelling behavior observation of the blend concludes the chitosan–starch blend cross-linked with CaCl_2 shows the highest swelling behavior at 10:10:2 mL concentration of starch, chitosan, and CaCl_2 . The antibacterial evaluation of the blends also shows that the blend having 10:10:2 mL concentration is effective against *E. coli*.

References

1. Çetinus, S.A., Sahin, E., Saraydin, D.: Preparation of Cu(II) adsorbed chitosan beads for catalase immobilization. *Food Chem.* **114**, 962–969 (2009)
2. Dutta, P.K., Tripathi, S., Mehrotra, G.K., Dutta, J.: Perspectives for chitosan based antimicrobial films in food applications. *Food Chem.* **114**(4), 1173–1182 (2009)
3. Chenite, A., Buschmann, M.D., Wang, D., Chaput, C., Kandani, N.: Rheological characterization of thermogelling chitosan/glycerol-phosphate solutions. *Carbohydr. Polym.* **46**, 39–47 (2001)
4. Kordestani S.S., Bahrami, S.B.: Chitin polymer for medical applications. In: Proc. of the Int. Sem. On Polym. Sci. & Technology, ISPST-97, Iran Polymer Institute, Vol II, pp. 742–747 (1997)
5. Xu, J., McCarthy, S.P., Gross, R.A.: Chitosan film acetylation and effects on biodegradability. *Macromolecules* **29**, 3436–3440 (1996)
6. Niamsa, N., Baimark, Y.: Preparation and characterization of highly flexible chitosan films for use as food packaging. *Am. J. Food Technol.* **4**, 162–169 (2009)
7. Teramoto, N., Motoyama, T., Yosomiya, R., Shibata, M.: Synthesis, thermal properties, and biodegradability of propyl-etherified starch. *Eur. Polym. J.* **39**, 255–261 (2003)
8. Zhang, J.-F., Sun, X.Z.: Mechanical properties of PLA/starch composites compatibilized by maleic anhydride. *Biomacromol* **5**, 1446–1451 (2004)
9. Araújo, M.A., Cunha, A., Mota, M.: Enzymatic degradation of starch-based thermoplastic compounds used in protheses: identification of the degradation products in solution. *Biomaterials* **25**, 2687–2693 (2004)
10. Ramesh, M., Mitchell, J.R., Harding, S.E.: Amylose content of rice starch. *Starch* **51**, 311–313 (1999)
11. Jie, R., Hongye, F., Tianbin, R., Weizhong, Y.: Preparation, characterization and properties of binary and ternary blends with thermoplastic starch, poly(lactic acid) and poly(butylene adipate-coterephthalate). *Carbohydr. Polym.* **77**, 576–582 (2009)
12. Singla, A.K., Chawla, M.: Chitosan: Some pharmaceutical and biological aspects – an update. *J. Pharm. Pharmacol.* **53**, 1047–1067 (2001)
13. Kumari, K., Rani, U.: Controlled release of metformin hydrochloride through crosslinked blends of chitosan-starch. *Pelagia Res. Libr. Adv. Appl. Sci. Res.* **2**(2), 48–54 (2011)
14. Giri, T.K., Thakur, A., Alexander, A., Ajazuddin, Badwaik, H., Tripathi, D.K.: Modified chitosan hydrogels as drug delivery and tissue engineering systems: present status and applications. *Acta Pharmaceutica Sinica B* **2**(5), 439–449 (2012)